Desalination and Water Treatment
www.deswater.com
doi: 10.5004/dwt.2023.29902

307 (2023) 105–119
September

Removal of nitrate ion from aqueous solutions by functionalization of nano clay: preparation, characterization and mechanistic performance

Homa Maleki[a], Giti Kashi[a,b,*], Nafiseh Nourieh[a], Rouhallah Mahmoudkhani[a]

[a]*Department of Environmental Health Engineering, Faculty of Health, Tehran Medical Sciences, Islamic Azad University, Tehran, Iran, emails: g.kashi@yahoo.com (G. Kashi), homamaleki75@gmail.com (H. Maleki), n.norieh@gmail.com (N. Nourieh), Mahmoodkhany@yahoo.com (R. Mahmoudkhani)*
[b]*Water Purification Research Center, Tehran Medical Sciences, Islamic Azad University, Tehran, Iran*

Received 18 May 2023; Accepted 23 August 2023

ABSTRACT

Nitrate, as one of the primary pollutants, is found in agricultural drainage water, and human and animal excrement. Nitrate causes damage to water environments and endangers human health. It is clear that the research is very important for the development and improvement of existing methods for treating water containing high concentrations of nitrate. This study was conducted aimed to investigate the possibility of using a batch system of nanoclay modified with the organic surfactant hexadecyltrimethylammonium bromide (HDTMA-Br) to remove nitrate anion as a model pollutant from drinking water containing this pollutant. This study was conducted on laboratory and batch reactor scale. Removal efficiency of different pH 4–9, contact time 15–60 min, nanoclay adsorbent concentration modified with organic surfactant HDTMA-Br 0.5–1.5 g/dL and nitrate concentration 25–75 mg/L was investigated. Nitrate concentration was measured by ultraviolet spectrophotometer. Based on the scanning electron microscopy, the particles have a uniform shape with high porosity and the diameter of the nanoclay particles modified using the organic surfactant HDTMA-Br was 1.6 nm. Based on the X-ray diffraction analysis, the modification process changed the base distance in the nanoclay structure from 17 to 24 Å. The best conditions for removal of 25 mg/L of nitrate (100% efficiency) included contact time of less than 15 min, optimum temperature of 20°C, optimum pH 4 and concentration of 1 g/dL of nanoclay modified using organic surfactant HDTMA-Br with the surface of the surfactant was 40% of the cation exchange capacity. The maximum nitrate adsorption capacity was 94.33 mg/g by following the Langmuir isotherm (correlation coefficient of 0.9960) and second-order adsorption kinetic (correlation coefficient of 0.9988). The results showed that the modified nanoclay adsorbent is a suitable, cheap and efficient method for removing nitrate from drinking water. Nanoclay adsorbent modified with the organic surfactant HDTMA-Br is used as a strong adsorbent to remove nitrate from aqueous media due to its high adsorption capacity and reusability for at least 4 cycles of recycling.

Keywords: Bentonite; Nanoclay adsorbent; Organic surfactant; Hexadecyl trimethyl ammonium bromide; Nitrate

1. Introduction

Nitrate (NO_3^-) is one of the primary pollutants that can be found in agricultural drainage water, human and animal excrement, and the untreated NO_3^- entering wastewater causes damage to aquatic environments and endangers the health of living organisms, especially humans [1,2]. NO_3^-, as an inorganic pollutant, is a very soluble and stable compound and can remain in the form of NO_3^- [3]. NO_3^-, with a nitrogen oxidation number of +5 and a negative charge,

* Corresponding author.

is easily washed from the soil by irrigation water and precipitation, moves to the ground water and causes its pollution [4]. NO_3^- reduction to nitrite by microorganisms under anoxic conditions can be a health risk for a person. The groups exposed to the health risk of NO_3^- include infants, pregnant women and children, and NO_3^- affects the thyroid gland [5]. Increasing the concentration of NO_3^- in drinking water is the cause of health challenges of infant methemoglobinemia (blue baby syndrome), especially 3–6 months old, and stomach cancer caused by nitrosamine compounds in adults [6,7]. Providing safe water is one of the most important priorities of the water supply industry. NO_3^- adsorption even below the maximum concentration (10 mg/L of nitrogen–nitrate) in water is considered harmful to human health, so NO_3^--contaminated water treatment is a strategic way to prevent excess water use and preventing endangering human life has been a high priority over the last few decades [8,9]. It is clear that the research is very important for the development and improvement of existing methods for treating water containing high concentrations of NO_3^- due to increasing removal efficiency. Many methods have been used and developed to remove NO_3^- more than the allowable limit, including the adsorption by ion exchange, reverse osmosis, adsorption, and chemical and biological methods [10]. Each of the methods mentioned above has advantages and disadvantages. Low removal efficiency, production of large volume of sludge, inefficiency of cost and energy, production of toxic by-products and spreading potentially more toxic chemicals in the environment are some of the disadvantages of using these methods [11]. The adsorption process has been used to remove NO_3^- from water over the last decade. The adsorption process has no problem mentioned [12]. In recent decades, the adsorption of NO_3^- by natural adsorbents has been considered due to economic efficiency. Some of these adsorbents are chitosan, coconut shell, bamboo, activated carbon, bentonite, zeolite, and sugarcane bagasse. The adsorption is the most effective and economical process for NO_3^- removal. In this method, biological adsorbents such as biomass, peat and biopolymer are used [13]. The high cost and problems associated with regeneration of saturated activated carbon adsorbent recently led to the development of clay adsorbent (bentonite) modified using cationic surfactants such as hexadecyltrimethylammonium bromide (HDTMA-Br. In order to removing different anions, different functionalized adsorbents have been used, such as 4-nitro-1-naphthylamine ligand functionalized porous conjugate material (mesoporous silica) for toxic NO_3^- detection and adsorption from wastewater [14]; the mesoporous silica and the 2-methyl-1-naphthylamine organic ligand composite adsorbent for phosphate adsorption from water [15]; 2-methyl-1-naphthylamine ligand on to porous silica for arsenic adsorption from contaminated water [16]; 1-naphthylamine ligand on to mesoporous silica for NO_3^- capturing from contaminated water [17]; *N*,*N*′-di(3-carboxysalicylidene)-3,4-diamino-5-ligand on to mesoporous silica monolith for the selective selenium monitoring and removal from water [18]; The adsorption capacity of clay modified with cationic surfactant can be attributed to the presence of hydroxide, carboxyl and silicon functional groups on the surface of modified clay and high specific surface area, high porosity, and positive charge of the adsorbent [19]. Chemical and mechanical stability is one of the advantages of clay adsorbent (bentonite as smectite nanoclay) modified using cationic surfactants such as HDTMA-Br. Nanoclays are very popular due to their high surface area, large pore volume, and high thermal stability modified using cationic surfactant HDTMA-Br [20]. The present study was conducted with regard to the crisis of water pollution to preserve water resources due to the widespread pollution of water resources caused by the uncontrolled discharge of urban, industrial and agricultural waste and the fulfilment of treatment standards. The adsorption technology by modified clay (bentonite) using cationic surfactant HDTMA-Br has been used as a new method to remove NO_3^- anions and achieve blue with good properties in accordance with standards. Among the smectite nanoclay, montmorillonite nanoclay have been studied by various researchers due to their abundance, compatibility with the environment, and good structure and chemical properties. Enkari and Ebrahimi [21] removed NO_3^- ions from aqueous solution using montmorillonite nanoclay modified using octadecylamine. Kang et al. [22] synthesized quaternary ammonium gel-silica functional group through dimethyldecyl binding [3-(trimethoxysilyl)propyl] ammonium chloride for NO_3^- removal in batch and column reactor studies. El Hanache et al. [23] modified nanozeolites using cationic surfactant HDTMA-Br as super-adsorbent to remove NO_3^- from polluted water. Treating water containing high concentrations of NO_3^-, the interpretation of the trend of NO_3^- concentration changes during the removal process and the factors affecting the removal process are among the innovative aspects of the research. Providing a basis for the efficiency of NO_3^- pollutant removal by clay nanoparticle adsorbents functionalized using cationic surfactant HDTMA-Br as a framework to improve the public health of society through the use of the study results for the purification of NO_3^- pollutants from the aquatic environment is the ideal objective of the research. The lower consumption of cationic surfactant, higher micro-porosity, and increasing the interlayer surface area compared to other studies shows the improvement of the current study method. The interpretation of the trend of NO_3^- concentration changes during the removal process and the factors affecting the removal process are among the innovative aspects of the research. Providing a basis for the efficiency of NO_3^- pollutant removal by clay nanoparticle adsorbents functionalized using cationic surfactant HDTMA-Br as a framework to improve the public health of society through the use of the study results for the purification of NO_3^- pollutants from the aquatic environment is the ideal objective of the research. This study was conducted aimed to investigate the possibility of using a discontinuous system of nanoclay modified using organic surfactant HDTMA-Br to remove NO_3^- anion from drinking water containing this pollutant.

2. Method

This study is a descriptive-cross-sectional experimental laboratory study, the statistical population of which is water samples contaminated with NO_3^-. The studied variables included NO_3^- removed under optimum conditions,

NO_3^- removal conditions such as time, pH, concentration of clay nanoparticles (B), cationic surfactant (HDTMA-Br) (H), clay nanoparticles functionalized using cationic surfactant HDTMA-Br. This study was conducted in a batch cylindrical glass reactor with the volume of 1,000 mL and effective volume of 500 mL. For proper mixing of the reactor, a plate shaker (100 rpm) was used. Nanoclay prepared without any pretreatment process was used during this research due to its high degree of purity (99.99%). To synthesize clay nanoparticles functionalized using cationic surfactant HDTMA-Br, the modified method of Singla et al. [24] was used. 5 g of bentonite nanoclay was added to 500 mL of distilled water and stirred using a magnetic stirrer for 22 h at 20°C. Over time, 2 g of cationic surfactant HDTMA-Br was added. The two were mixed for 13 h and filtered using filter paper. After filtering the solution, the precipitate was heated at 85°C for 200 min.

To investigate the surface, shape, size, and placement of particles on the cationic surfactant HDTMA-Br, scanning electron microscopy (SEM; Philips XL30, Holland) and X-ray diffraction (XRD; Rigaku Instrument Corporation, Japan) were used to identify the structure of modified nanoparticles.

Chemical variables were measured based on the instructions of the standard method book. 1,000 mg/L of synthetic NO_3^- solution was prepared by dissolving 1.5 g of Merck potassium NO_3^- powder (dried at 103°C for 60 min) in 1,000 mL of deionized water. By diluting, 25, 50 and 75 mg/L of NO_3^- was obtained. Tests were performed to determine the process efficiency at 3 initial NO_3^- concentrations 25, 50 and 75 mg/L, 3 reaction times 15, 30 and 60 min, different pH 4, 6.5 and 9 and 3 nanoparticle adsorbents clay, cationic surfactant (H) and clay nanoparticles functionalized using cationic surfactant (H) 0.5, 1 and 1.5 mg/dL for optimum determination of variables in batch reactor (adsorbents of clay nanoparticles, cationic surfactant (H), clay nanoparticles functionalized using cationic surfactant (H) at laboratory temperature. After adjusting the pH in the corresponding batch reactor, 500 mL of synthetic sample with adsorbents of clay nanoparticles, cationic surfactant (H), clay nanoparticles functionalized using cationic surfactant (H) was poured and the shaker was turned on at the desired reaction times. Over time, 25 mL of water sample was taken from the middle of the reactor for testing, passed through a filter of 0.45 microns, the remaining NO_3^- concentration was read at 220 nm using an ultraviolet spectrophotometer, and the correlation coefficient was at least 0.995, confirming the drawn NO_3^- standard curve. After ensuring the accuracy of the ultraviolet spectrophotometer, the lowest standard solution was added to it and the lowest accuracy of the standard reading was considered as the detection limit, which is equivalent to 3 times the amount of interference created in the control chart (0.04 mg/L). 10 times the amount of interference was considered as the measurement range. Also, for the accuracy, 3 samples were prepared and placed in the UV spectrophotometer at different times (3 times) and checked in 3 d, until finally the accuracy of the method was confirmed. The number of samples was obtained from the method of designing tests of 90 samples. Data were analyzed using Excel and SPSS version 18, which included *t*-test and chi-square test for the quantitative and qualitative variables. NO_3^- removal efficiency is calculated by the following equation:

$$\text{Removal}(\%) = 1 - \frac{C_t}{C_{to}}$$

where C_t is the NO_3^- concentration after the adsorption process at time t and C_{t0} is the initial NO_3^- concentration at time t_0.

In view of application, Taguchi model for optimizing is very applicable for rapid assessment of optimal conditions based on a small number of tests and is effective for more than one process parameter. In addition, the Taguchi model was utilized to represent the relationship between four operational variables (adsorbent concentration as factor 1; pH as factor 2; NO_3^- concentration as factor 3; reaction time as factor 3) and three levels of removal efficiency. Therefor a new set of 9 experiments was conducted.

3. Results and discussion

Factors affecting the efficiency of organic bentonite adsorbent (clay nanoparticles functionalized using cationic surfactant (H)) are: surface morphology by SEM, long distance between layers due to organization by XRD, creating hydrophobic property by Fourier-transform infrared spectroscopy (FTIR), long distance between layers in acidic pH, limitation of adsorption active sites on to adsorbent due to increasing initial NO_3^- concentration, increasing the contact surface with the NO_3^- and creating more absorption sites due to increasing adsorbent concentration, reaction time, temperature, adsorbent stability (reusability).

3.1. Modified nanoclay structure

To determine the crystalline properties and purity of clay nanoparticles, cationic surfactant (H), and clay nanoparticles functionalized using cationic surfactant (H), XRD was used. The output peaks at supplementary angles equal to 7.26° and 21.87° are consistent with the standard peaks of montmorillonite (equivalent to 001 and 100) and thus confirm the purity (Fig. 1). Illite, quartz, kaolinite, cristobalite impurity was identified according to the peaks indicated. Silica, aluminum, oxygen and sodium are considered as main elements (Fig. 2 and Table 1). As shown, the amount of carbon and nitrogen have increased due to the penetration of cationic surfactant H in the surface of bentonite, and the amount of calcium, sodium and magnesium have reduced due to the exchange of cations between sodium, calcium and magnesium and the alkyl chain. The presence of sharp and narrow peaks indicates the crystallinity of the synthesized samples. The output peaks at two angles equal to 7.26° and 21.87° are consistent with the standard peaks of montmorillonite (equivalent to 001 and 100). The supplementary bentonite pattern (2°–10°) has a distinct peak at 7°, indicating that the silicate d-layer spacing (distance) is 1.2 nm. Therefore, the purity of the nanoparticle is confirmed. The results showed that bentonite layers expanded due to modification using surfactant that contained a long-chain alkyl group [25]. In the modification of montmorillonite with cationic surfactant (H), the interlayer distance is reduced from 7.26° to 21.87° due to the entry of organic materials into the montmorillonite layers which indicates the organization

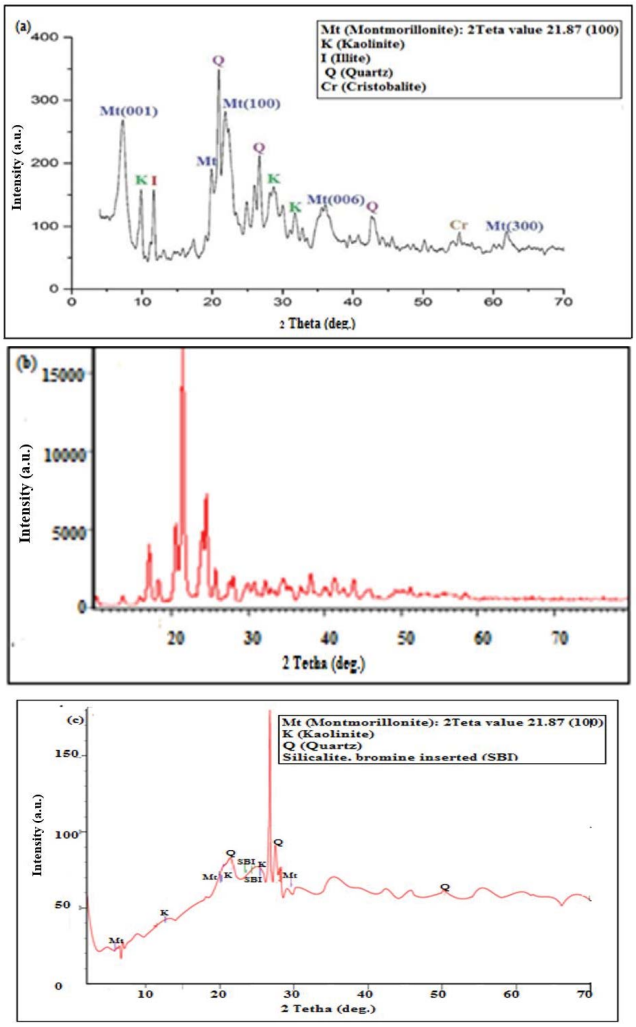

Fig. 1. X-ray diffraction image: (a) bentonite nanoparticles, (b) cationic surfactant H, and (c) clay nanoparticles functionalized using cationic.

of bentonite and leads to producing organic bentonite absorbent.

SEM was used to determine the structure of clay nanoparticles, cationic surfactant H, and clay nanoparticles functionalized using cationic surfactant H (Fig. 3). The raw clay nanoparticles have an irregular, multi-layered lumpy shape with high porosity, and the minimum particle diameter of 7.33 nm. High surface area helps to increase NO_3^- adsorption capacity on clay nanoparticles. Clay nanoparticles functionalized using cationic surfactant H have a more uneven shape with cracked layers and a minimum particle diameter of 0.2 nm. The roughness of the surface, high porosity due to the porous structure and large surface area help to increase the capacity of NO_3^- adsorption on clay nanoparticles [26]. SEM micrographs showed that this increase in clay improvement content causes more compatibility between the filler layers and increases the adsorption capacity. Modifying the surface of clay nanoparticles has led to different effects on clay nanoparticles, which in the first stage includes increase in

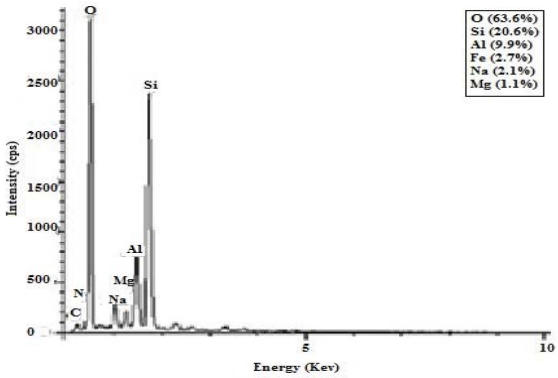

Fig. 2. Percentage of nanoclay elements analyzed by energy-dispersive X-ray spectroscopy.

Table 1
w/w% of elements of clay nanoparticles functionalized using cationic surfactant H

No.	Element	w/w%
1	Carbon	11.3
2	Nitrogen	1.14
3	Magnesium	0.97
4	Calcium	0.42
5	Sodium	0.21

adsorption due to increase in porosity, increasing the surface of nanoparticles, increasing the surface available for the adsorption of NO_3^- anions, and increasing the removal efficiency due to increasing the number of adsorption sites. There are van der Waals force, electrostatic force or hydrogen bonds between the layers of montmorillonite. The presence of interlayer spaces can be increased by cationic surfactants due to exchanging cations with the surface in the nanoclay layers which increases the adsorption sites.

Infrared spectroscopy was used to determine the structure of clay nanoparticles, cationic surfactant H, clay nanoparticles functionalized using cationic surfactant H (Fig. 4). The peak bands of bentonite nanoparticles include 471; 609; 179; 1,046; 1,638; 3,437 and 3,738 cm, respectively, belonging to Si–O–Si bending vibration, Si–O–Al bending vibration, quartz, Si–O stretching vibration, bending vibration of water molecule adsorbed on bentonite, stretching vibration of water molecule adsorbed on bentonite and O–H stretching vibration. The peak bands of cationic surfactant nanoparticles H include 2,919 and 2,851 cm, respectively, belonging to the symmetric and asymmetric bonds of methyl and methylene stretching vibrations. Table 2 shows the properties of clay nanoparticles, cationic surfactant H, clay nanoparticles functionalized using cationic surfactant H. The maximum specific surface area of bentonite was 28.99 m^3/g.

$–CH_2$ and $–CH_3$ vibrations show the existence of long alkyl chain in bentonite. According to the modifications of the adsorbent, the functional groups in the spectrum provided by FTIR were confirmed and the chemical structure of the adsorbent was qualitatively evaluated as good. This result was also reported by other researchers [27]. The

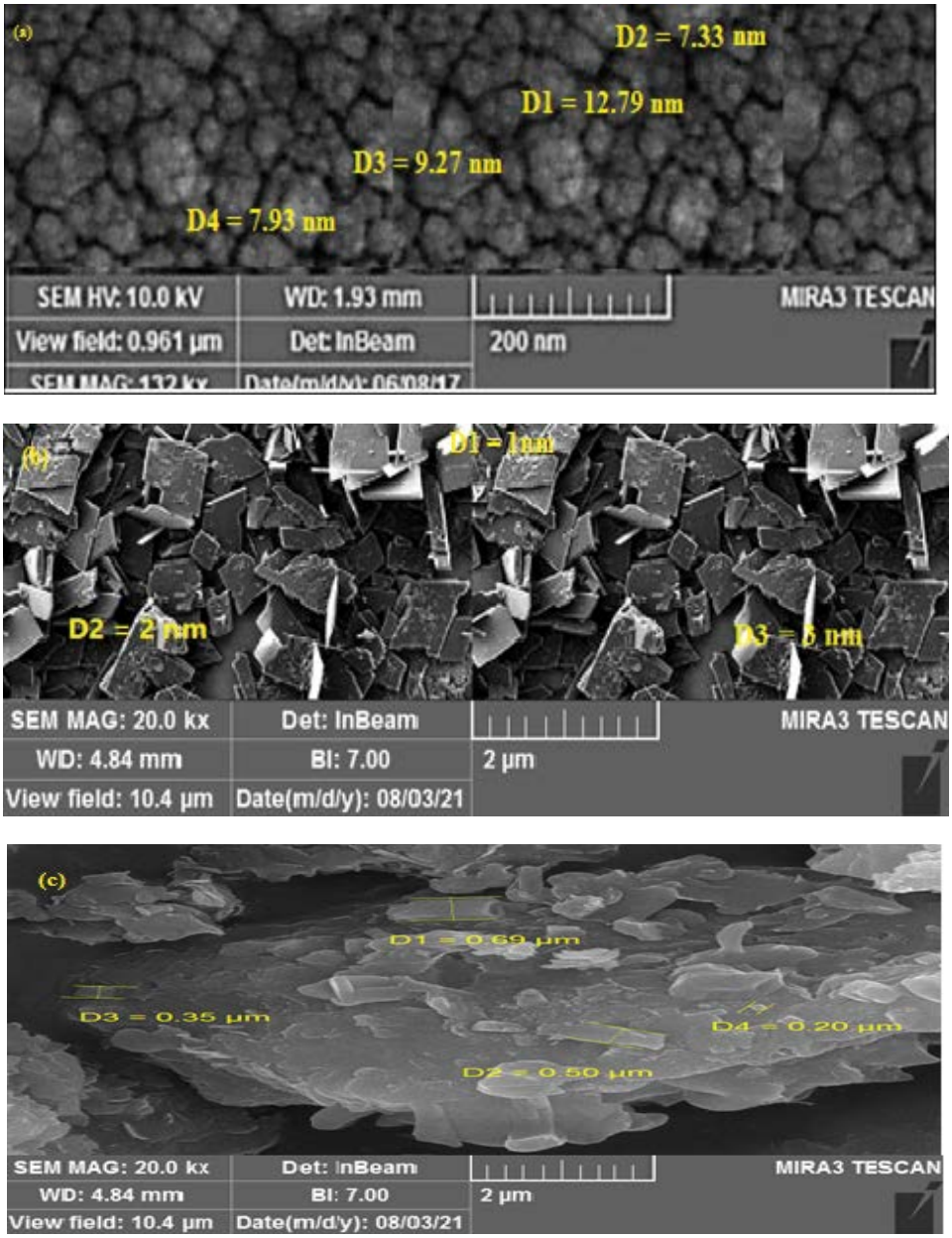

Fig. 3. Scanning electron microscopy image: (a) bentonite nanoparticles, (b) cationic surfactant H, and (c) clay nanoparticles functionalized using cationic surfactant H (200 kV).

maximum specific surface area of the adsorbent of clay nanoparticles, cationic surfactant H, functionalized nanoclay using cationic surfactant H was 33.65, 0.38 and 1.17 m^2/g, respectively. The structure of the modified nanoparticle based on BET theory showed that the changes in the nanoparticle after modification caused a reduction in the volume and surface area of the pores and an increase in adsorption due to the presence of functional groups. But the diameter of modified nanoparticle was more. Rathnayake et al. [28], by investigating the specific surface area of mineral and organic clay and modifying clay by HDTMA-Br, showed that the specific surface area and pore volume reduced due to the occupation of the interlayer space of clay particles by the surfactant, and an increase in diameter and adsorption showed the presence of functional groups.

3.2. Effect of pH on NO_3^- adsorption

The efficiency of the NO_3^- removal process of clay nanoparticles, cationic surfactant H, clay nanoparticles functionalized using cationic surfactant H increases at pH 4 and 25–75 mg/L of NO_3^-. pH 4 needs a lower concentration of adsorbent compared to the other two. This can be attributed to the active adsorption sites in the surface and deep parts of the absorbers. A reduction in pH has led to an increase in the adsorption rate. The lowest amount of remaining

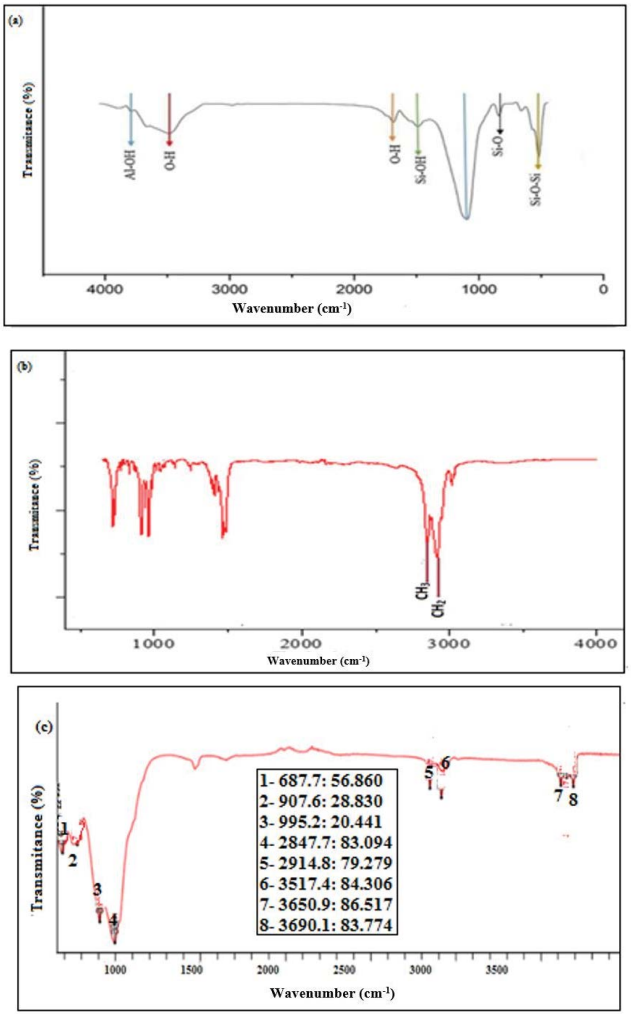

Fig. 4. Fourier-transform infrared spectroscopy image: (a) bentonite nanoparticles, (b) cationic surfactant H, and (c) clay nanoparticles functionalized using cationic surfactant H (before adsorption). Notes: In the FTIR spectrum related to the absorption of NO_3^- anions by the adsorbent (clay nanoparticles functionalized using cationic surfactant), the peaks were observed at the wavenumber 693.2 (57.29), 910.4 (28.91), 1,007.5 (20.69), 2,848.9 (83.12), 2,924.3 (79.53), 3,527.4 (84.54), 3,651.5 (86.5), 3,691.9 (83.81), respectively.

NO_3^- (100% NO_3^- removal efficiency) was at pH 4, reaction time of 60 min, 25 mg/L of NO_3^- and 2 g/dL of adsorbent of clay nanoparticles. The lowest amount of remaining NO_3^- (22.5% NO_3^- removal efficiency) was at pH 4, reaction time of 60 min, 25 mg/L of NO_3^- and 2 g/dL of adsorbent of cationic surfactant H. The lowest amount of residual NO_3^- (100% NO_3^- removal efficiency) was at pH 4, reaction time 30 min, and clay nanoparticles functionalized using cationic surfactant H (Fig. 5 and Tables 3–8). One of the most important effective factors in the adsorption of NO_3^- pollutant on the absorbent surface is the initial pH of the solution. The initial pH of the solution can affect the surface charge of the adsorbent and change the state of the pollutant in the aqueous environment. The initial pH of the solution determines the surface properties of the adsorbent and the adsorbed material. Determining the pH point of zero charge (pH_{zpc}) leads to the interpretation of the amount of NO_3^- adsorption due to the surface charge of the adsorbent at different pH. The pH_{zpc} value of adsorbents of clay nanoparticle, and functionalized nanoclay using cationic surfactant H was obtained as 7.4 and 8, respectively, indicating neutral conditions. In this study, the best pH for NO_3^- adsorption was found to be 4, which has the highest adsorption capacity for NO_3^- anion. Because at this pH, the available NO_3^- is turned into nitrite ion, which has better adsorption than the NO_3^- molecule

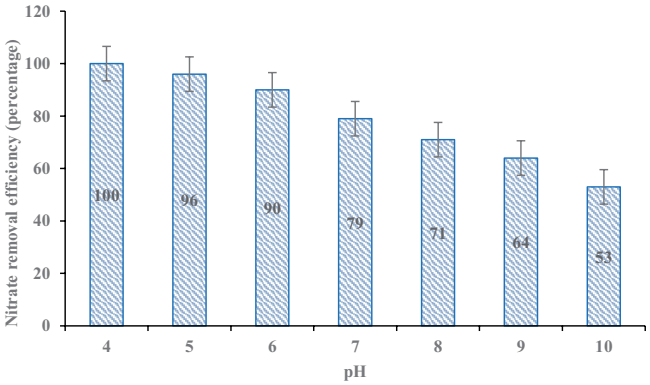

Fig. 5. Effect of pH on NO_3^- adsorption (optimum conditions of clay nanoparticles functionalized using cationic surfactant H: reaction time of 60 min, 25 mg/L of NO_3^-, and 2 g/dL of adsorbent of clay nanoparticles).

Table 2
Properties of bentonite nanoparticles, cationic surfactant H, clay nanoparticles functionalized using cationic surfactant H

Unit	Nanoparticles		
	Bentonite	Cationic surfactant	Clay nanoparticles functionalized using cationic surfactant
Total net volume (cm^3/g)	7.73	0.09	0.012
pH_{zpc} (–)	7.4	–	8
Specific surface area (m^2/g)	33.65	0.38	1.17
Diameter (nm)	7.33	39.3	40.57
Zeta potential (mV)	–50.3	–53.1	–20.2
Barrett–Joyner–Halenda, BJH (nm)	4.03	2.38	1.85
Cation exchange capacity (meq/100 g)	108.4	23	120.6

Table 3
Results of the effect of bentonite on NO_3^- removal from drinking water (25, 50 and 75 mg/L, pH 4, and different contact times and amounts of bentonite adsorbent)

Bentonite adsorbent concentration (g/dL)	Removal efficiency percentage 25 mg/L			Removal efficiency percentage 50 mg/L			Removal efficiency percentage 75 mg/L		
	Time (min)			Time (min)			Time (min)		
	15	30	60	15	30	60	15	30	60
1	52	60	57	42	50	47	32	40	37
2	63	70	100	53	60	80	43	50	70
3	58	65	72	48	55	62	38	45	52

Table 4
Results of the effect of bentonite in removing NO_3^- from drinking water (25, 50 and 75 mg/L, pH 6.5, and different contact times and amounts of bentonite adsorbent)

Adsorbent (g/dL)	Removal efficiency percentage 25 mg/L			Removal efficiency percentage 50 mg/L			Removal efficiency percentage 75 mg/L		
	Time (min)			Time (min)			Time (min)		
	15	30	60	15	30	60	15	30	60
1	47	55	62	37	45	52	27	35	42
2	58	65	73	48	55	63	38	45	53
3	53	60	67	43	50	57	33	40	57

Table 5
Results of the effect of bentonite in removing NO_3^- from drinking water (25, 50 and 75 mg/L, pH 9, and different contact times and amounts of bentonite adsorbent)

Adsorbent (g/dL)	Removal efficiency percentage 25 mg/L			Removal efficiency percentage 50 mg/L			Removal efficiency percentage 75 mg/L		
	Time (min)			Time (min)			Time (min)		
	15	30	60	15	30	60	15	30	60
1	42	47	60	32	37	40	22	27	30
2	53	58	68	43	48	50	33	38	40
3	48	52	55	38	42	45	28	32	35

Table 6
Results of the effect of cationic surfactant (H) in removing NO_3^- from drinking water (25, 50 and 75 mg/L, pH 4, and different contact times and amounts magnetic nanoparticles)

Adsorbent (g/dL)	Removal efficiency percentage 25 mg/L			Removal efficiency percentage 50 mg/L			Removal efficiency percentage 75 mg/L		
	Time (min)			Time (min)			Time (min)		
	15	30	60	15	30	60	15	30	60
20	18	19	17	14.0	17	16	12	16	14.0
40	20	22	21.5	18.5	20	19.5	17	19	18
60	17.5	21	19.5	16.5	18	17.5	14.5	17	16.5

[29]. pH 4 requires a lower concentration of adsorbent compared to the other two, which can be attributed to the active site of adsorption in the surface and deep parts of the adsorbent. An increase in pH leads to a reduction in positive charge and adsorption of NO_3^- [30]. Clay nanoparticles have a positive charge at low pH and absorb anionic ions

Table 7
Results of the effect of cationic surfactant H in removing NO_3^- from drinking water (25, 50 and 75 mg/L, pH 6.5, and different contact times and amounts)

Adsorbent (g/dL)	Removal efficiency percentage 25 mg/L			Removal efficiency percentage 50 mg/L			Removal efficiency percentage 75 mg/L		
	Time (min)			Time (min)			Time (min)		
	15	30	60	15	30	60	15	30	60
20	14.0	17	15	12.0	15	14	12	14	12.0
40	18	20	19.5	16.5	18	17.5	15	17	16
60	15.5	19	17.5	14.5	16	15.5	12.5	15	14.5

Table 8
Results of the effect of cationic surfactant H in removing NO_3^- from drinking water (25, 50 and 75 mg/L, pH 9, and different contact times and amounts of magnetic nanoparticles)

Cationic surfactant HDTMA-Br (%)	Removal efficiency percentage 25 mg/L			Removal efficiency percentage 50 mg/L			Removal efficiency percentage 75 mg/L		
	Time (min)			Time (min)			Time (min)		
	15	30	60	15	30	60	15	30	60
20	7	17	15	5.0	15	14.0	2	3.0	7.0
40	18	20	19.5	16.5	18	17.5	15	17	16
60	15.5	19	17.5	14.5	16	15.5	7.0	15	14.5

such as NO_3^- more. Increasing the pH to more than pH_{zpc} leads to a reduction in NO_3^- adsorption due to the electrostatic repulsion force in the adsorbent surface. Due to the negative charge of chloride ion, the electrostatic force between chloride and hydroxyl ions increases the probability of chloride adsorption. Another researcher reported the highest removal efficiency of NO_3^- from water using montmorillonite was modified by hexadecyl trimethyl- at optimum pH 5.4 [31]. Another researcher reported the highest removal efficiency of lead from contaminated water using the chemical ligand-based conjugate adsorbent at optimum pH 3.5 [32].

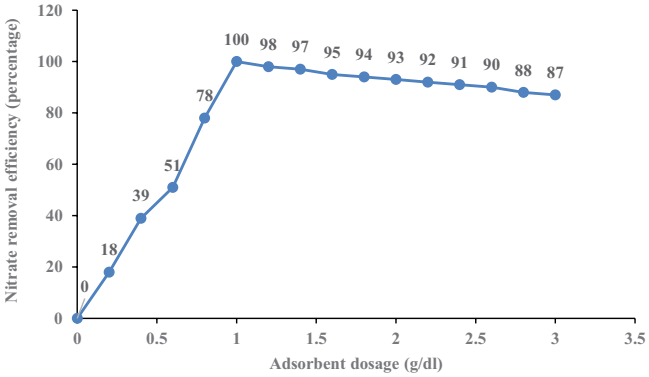

Fig. 6. Effect of the amount of adsorbent on NO_3^- adsorption (optimum conditions of clay nanoparticles functionalized using cationic surfactant H: reaction time of 60 min, 25 mg/L of NO_3^-, and pH 4).

3.3. Effect of the amount of adsorbent

Increasing the concentration of clay nanoparticles, cationic surfactant H, clay nanoparticles functionalized using cationic surfactant H increased NO_3^- removal efficiency. Increasing the adsorbent concentration of clay nanoparticles from 1 to 2 g/dL with pH 4, reaction time of 60 min, 25 mg/L of NO_3^- increased the removal efficiency percentage from 18% to 100%. The increase in the amount of adsorbent led to an increase in the adsorption capacity due to the increase in the number of active sites on the adsorbent surface. Increasing the concentration of cationic surfactant adsorbent H from 20% to 40% with pH 4, reaction time of 60 min, and 25 mg/L of NO_3^- increased removal efficiency percentage from 15% to 19.5%. Increasing the adsorbent concentration of functionalized clay nanoparticles using cationic surfactant H from 1 to 2 g/dL with pH 4, reaction time of 30 min, 25 mg/L of NO_3^- increased the removal efficiency percentage from 98% to 100% (Fig. 6 and Tables 3–8). Increasing the amount of the adsorbent increased the percentage of NO_3^- removal, which is due to the increase in the specific surface area of the adsorbent, the contact surface, and the direct contact between the active sites of the adsorbent of clay nanoparticles, cationic surfactant HDTMA-Br, nanoclay functionalized using cationic surfactant H and NO_3^- anion. By increasing the amount of adsorbent dose from 1 to 2 g/dL, adsorption also increased, due to increasing the progressive forces in the value of 2 g/dL than the initial doses of nano-absorbent, which causes all the adsorption sites to be quickly absorbed by NO_3^- anions. By increasing the amount of adsorbent, as one of the effective parameters in increasing the efficiency of

adsorption, the exchange surface available for the equilibrium adsorption that is available to the adsorbed substance is increased. The higher the ratio of the surface to the volume of the nanoparticle, the greater the reactivity, and increasing the adsorbent dose by increasing the contact surface between the pollutant and creating more sites for pollutant adsorption, increases the efficiency of the pollutant adsorption process but after the amount of 2 g/dL of nano-absorbent, the transfer of NO_3^- ions on the surface of modified clay nanoparticles has a constant amount of NO_3^- adsorption efficiency due to the lack of active sites. Modified nanoclay in lower concentration and reaction time can carry out the process of NO_3^- anions adsorption compared to pure clay which shows the adsorption power of modified nanoclay compared to pure clay. It is concluded that the functional group of the cationic detergent on the surface of the absorbent can be suitable for absorbing NO_3^- groups and suitable places for it to be absorbed next to the nanoclay, and the reason for increasing the amount of NO_3^- anions adsorption compared to pure nanoclay. The study results of the effect of the amount of the adsorbent showed that by increasing the concentration of all three adsorbents to remove NO_3^- from 1 to 2 g/dL with pH 4, respectively, reaction times of 15, 30 and 60 min, and 25 mg/L of NO_3^- increased the removal efficiency from 18% to 100%, 15% to 19.5%, and 98% to 100%, and the adsorption capacity from 2.25 to 12.5, 1.87 to 2.43, and 12.25 to 12.5 mg/g, respectively. Another researcher reported that Nano bentonite was able to adsorb about 78.3% and 100% for initial concentrations of 100 and 20 mg/L, respectively [33]. Another study reported an increase in direct yellow 50 removal efficiency from 78% to 100% by adding 0.2 g of hexadecyltrimethylammonium bromide into the pure bentonite adsorbent [34]. An increase in the amount of the adsorbent increased the number of active adsorbent adsorption sites of NO_3^- anion on zinc. An increase in the amount of the adsorbent increased the efficiency removal of Europium on hybrid conjugate material [35].

3.4. Effect of the amount of reaction time

Increasing the concentration of NO_3^- from 25 to 75 mg/L with pH 4 leads to an increase in the contact time from 30 to more than 60 min for 100% removal. The lowest amount of NO_3^- remaining (100% NO_3^- removal efficiency), pH 4, 25 mg/L of NO_3^- and 2 g/dL of adsorbents of clay nanoparticles and clay nanoparticles functionalized with cationic surfactant H was related to 60 and 30 min, respectively (equilibrium time). Increasing the reaction time from 0 to 20 min increased the efficiency strongly (Fig. 7 and Tables 3–8). The rapid increase in removal efficiency in the first few min was attributed to the active sites on the adsorbent surface. The contact time is an important parameter for the use of adsorption, and increasing the contact time of the adsorbent with the pollutant increases the probability of trapping the pollutant and the efficiency of the process will increase until the saturation of the adsorbent. This increasing trend gradually reduced and reached a fixed point (equilibrium point) where the amount of adsorption and desorption was in a constant range and the efficiency did not change. The maximum removal of NO_3^- in the first 30 min of observation and up to the contact time of 60 min has a constant trend. The increase in adsorption efficiency in the initial times is due to the larger surface area, many empty sites, high reactivity and the higher availability of the absorbent of binding sites near the surface of clay, but after reaching the equilibrium time, the vacancy sites on the absorbent surface are occupied by NO_3^- anions and the efficiency follows a constant trend. Another researcher reported that bentonite pretreatment with acid led to increasing the adsorptive removal of ciprofloxacin from water in less time [36,37]. Another researcher reported that the adsorption of copper on to clay increased rapidly over time (in the first 30 min) and reached saturation in approximately 120–240 min [38]. Another researcher showed that the amount of nickel ions adsorbed on to clay enhanced with enhanced contact time and that equilibrium adsorption was reached in 15 min [39]. The increase in NO_3^- removal efficiency did not occur in 40–90 min and the adsorbent contact time was 30 min. NO_3^- anion removal on nanoclay functionalized using H cationic surfactant is a fast process because about 93% of NO_3^- anion removal occurs in the first 20 min, indicating its power. The study results are consistent with the results of other studies [40].

3.5. Effect of the amount of NO_3^- concentration

An increase in NO_3^- concentration reduced the efficiency of NO_3^- removal. Increasing the concentration of NO_3^- from 25 to 75 mg/L with pH 4, reaction time of 60 min, and 2 g/dL of nanoclay adsorbent reduced the removal efficiency from 100% to 70% and an increase in the adsorption capacity from 12.5 to 8.75 mg/g. Increasing the concentration of NO_3^- from 25 to 75 mg/L with pH 4, reaction time of 30 min and 2 g/dL of the adsorbent of clay nanoparticles functionalized using cationic surfactant H reduced the removal efficiency from 100% to 67% and increases the adsorption capacity from 12.5 to 12 25 mg/g. The increase in NO_3^- concentration reduced the efficiency of NO_3^- removal due to the reduction in the number of active sites on the adsorbent surface due to the saturation of the active sites (Fig. 8 and Tables 3–8). The pollutant removal mechanism depends on its initial concentration. At optimum concentration (25 mg/L), NO_3^- anions

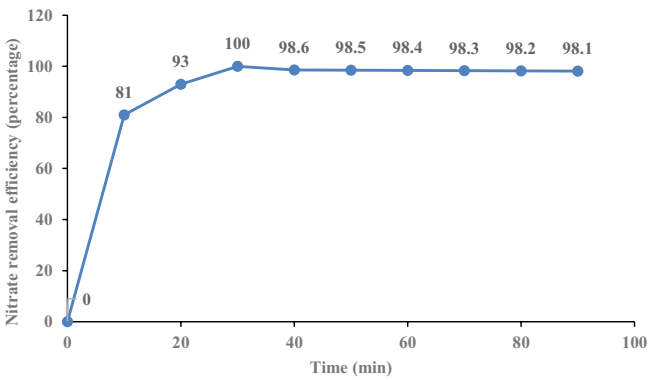

Fig. 7. Effect of reaction time on NO_3^- adsorption (optimum conditions of clay nanoparticles functionalized using cationic surfactant HDTMA-Br).

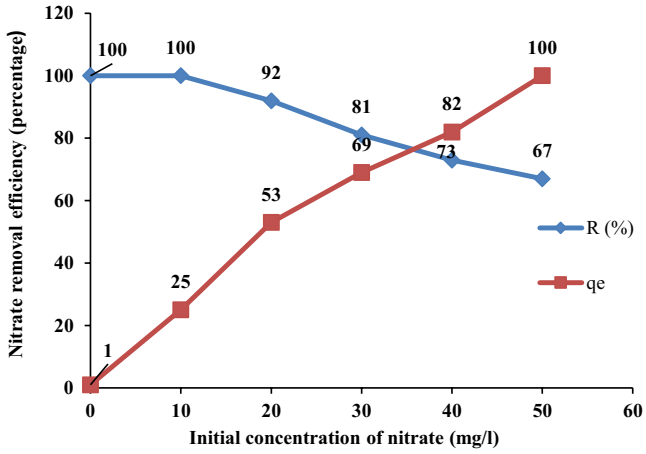

Fig. 8. Effect of initial concentration on NO_3^- adsorption (optimum conditions of clay nanoparticles functionalized using cationic surfactant H).

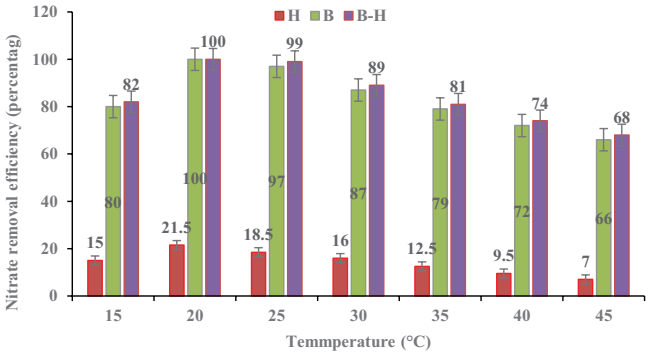

Fig. 9. Effect of temperature on NO_3^- adsorption (optimum conditions). Notes: The reaction time in bentonite adsorbent (B), cationic surfactant (HDTMA-Br) (H) and clay functionalized using cationic surfactant (HDTMA-Br) (B-H) is 60, 60 and 30 min, respectively.

are first absorbed in special adsorption sites and then in exchange sites due to the saturation of the special adsorption sites to achieve the highest adsorption rate, but after this adsorption rate, as the concentration increases, the removal efficiency also decreases. NO_3^- removal in terms of time is proportional to the NO_3^- anion concentration of the water. There are sufficient active sites for adsorption at low NO_3^- concentration, which increase the probability of contact between the adsorbent and the adsorbed. The reduction in adsorption efficiency is related to the increase in NO_3^- concentration with the ratio of NO_3^- concentration to the available surface of the adsorbent. Increasing the initial concentration of NO_3^- reduced the adsorption efficiency and an increase in the adsorption capacity due to the increase in the interaction between NO_3^-, adsorption sites, concentration gradient and driving force [41]. NO_3^- removal efficiency by the oak leaf adsorbent reduced the adsorption efficiency from 94.41% to 89.35% by increasing the initial concentration of NO_3^- from 5 to 120 mg/L [42]. Remazol Brilliant Red F3B removal efficiency by chitosan-treated cotton composite reduced by increasing the initial concentration of Brilliant Red F3B [43].

3.6. Effect of temperature

Fig. 9 shows the effect of temperature on NO_3^- removal efficiency. Increasing the temperature from 15°C to 20°C leads to an increase in NO_3^- removal efficiency from 82% to 100% due to the exothermic nature of the process. The sorption amount enhanced with an enhance in temperature [44]. Bentazon removal by the surfactant-modified pillared montmorillonites using cetyltrimethylammonium bromide adsorbent showed that the maximum adsorption capacity was occurred at room temperature [45]. NO_3^- removal reaction by clay nanoparticle adsorbent functionalized using cationic surfactant H is possible at room temperature. A reduction in NO_3^- removal efficiency in the temperature range of 30°C–45°C is due to the weaker gravity between the NO_3^- cation and surface-active sites on the clay nanoparticle adsorbent functionalized using cationic surfactant H. An increase in temperature leads to an increase in the speed of movement of NO_3^-, the active sites of adsorption and the collision of NO_3^- anion with the adsorbent surface, and a reduction in time for the interaction between the active sites of the adsorbent and absorbed NO_3^-. The reduction in NO_3^- removal efficiency in the temperature range of 30°C–45°C is due to the weakening gravity between the NO_3^- anion and the surface-active sites on the clay nanoparticle adsorbent functionalized using cationic surfactant H. An increase in temperature leads to an increase in the movement speed of NO_3^- and there is less time for interaction between the active sites of the adsorbent and the adsorbed NO_3^-. Each adsorbent can have its own optimum temperature so that the adsorption rate is better. Therefore, the factor of temperature depends on the type of absorber. The optimum temperature during the equilibrium contact time for 4-chlorophenol and 2,4-dichlorophenol adsorption by organoclays-with dodecyltrimethylammonium bromide (DTAB) and cetyltrimethylammonium bromide (CTAB) was 35°C [46]. The maximum removal of desulfurization of oil on organoclay-dibenzothiophene adsorbent was at 45°C [47]. An increase in temperature leads to an increase in NO_3^- mobile due to enlarging of adsorbent pores and reducing the activation energy [48]. A reduction in temperature leads to a reduction in NO_3^- adsorption due to a decrease in the availability of NO_3^- to the active sites on the absorbers of clay nanoparticles, cationic surfactant H, and nanoclay functionalized using cationic surfactant H due to a reduction in molecular vibration. Thermogravimetric analysis (TGA) curves of nanoclay and clay nanoparticle adsorbent functionalized using cationic surfactant H are performed in the temperature range of 20°C–1,000°C. The first, second, and third degradation for clay nanoparticle adsorbent functionalized using cationic surfactant H are seen at 100.84°C, 345.80°C, and 641.79°C, respectively. The first, second, and third degradation for nanoclay are seen at 269.63°C, 388.32°C, and 657.45°C, respectively. In the adsorption literature, the Van't Hoff equation is used for calculation of thermodynamic parameters of adsorption [49].

3.7. Effect of adsorbent reusability and regeneration study

Fig. 10 shows the effect of adsorbent reusability on NO_3^- removal. The efficiency reduced from 100% in the first use to 63% in the tenth use due to the reduction in active sites and their deactivation on the surface of the adsorbent, indicating the high power of the adsorbent in its repeated use. No significant reduction was in NO_3^- removal efficiency until the forth use. Economically, the use of cationic surfactant (H)-functionalized clay nanoparticles adsorbent for at least 4 times is economical due to the adsorbent reusability with high removal efficiency. Increasing the number of uses from the first time to the tenth time led to a reduction in NO_3^- removal efficiency due to a reduction in the number of active sites on the adsorbent surface. The study results are consistent with the results of other studies [50]. The cationic surfactant (H)-functionalized clay nanoparticles adsorbent after at least forth use is regenerated by HCl solution of o.1 N and fallowed by adding cationic surfactant (H) as a functional agent.

3.8. Equilibrium adsorption isotherms

The reason for choosing two isotherms of Langmuir and Freundlich to match the equilibrium experimental data with different mathematical models (adsorption isotherm modeling) is to interpret the surface adsorption behavior on the nano-absorbent. The data of adsorption isotherm tests, the analysis of these data, and the determination of the adsorption isotherm model are necessary for the design of adsorption process units. Table 9 shows the results of Langmuir NO_3^- adsorption isotherm. The maximum adsorption capacity of a single layer for NO_3^- anions is 94.33 mg/g. The correlation of 0.9969 of the Langmuir model, as a high anion is 94.33 mg/g. The correlation of 0.9969 of the Langmuir model, as a high value of correlation coefficient, shows the uniform monolayer adsorption on the adsorbent surface of clay nanoparticles functionalized using cationic surfactant (H), adsorbent power and high adsorption capacity, and indicating the desirability of the adsorption process (Table 9). The value of Freundlich's constant (coefficient of heterogeneity) 43.51 $(mg/g)(L/mg)^{1/n}$ and the correlation coefficient is 0.927, indicating the optimum adsorption of multilayers on different active sites with different energy levels. NO_3^- anions with different energy levels are kept on the adsorbent of clay nanoparticles functionalized using cationic surfactant (H) due to the energy inequality between the adsorption sites and NO_3^- anions. Isotherm studies provide important information for the design of pollutant adsorption processes in the liquid phase [51]. The equilibrium adsorption data were analyzed using Langmuir–Freundlich isotherm models to understand the adsorbent–adsorption interactions. The adsorption usually takes place on flat surfaces that have a fixed number of similar sites and each site can only absorb one anion. The Freundlich model shows that the binding energy reduces exponentially by increasing surface saturation. The adsorption isotherm of the Freundlich model shows the optimum adsorption of multilayers [52]. The removal of NO_3^- by clay nanoparticles functionalized using cationic surfactant H follows the Langmuir model adsorption equilibrium isotherm. This means that the adsorption has happened as a single layer and the same. Accordingly, the maximum NO_3^- adsorption capacity was 33.94 mg/g, indicating the high adsorbent capacity of clay nanoparticles functionalized using cationic surfactant H to remove NO_3^-. The NO_3^- adsorptive from water on nanoclay and organo-nanoclay adsorbents fitted with the Langmuir model and showed homogeneous surface connection [53]. The removal of lutetium by organic ligand-based sustainable composite hybrid material followed the Langmuir model adsorption

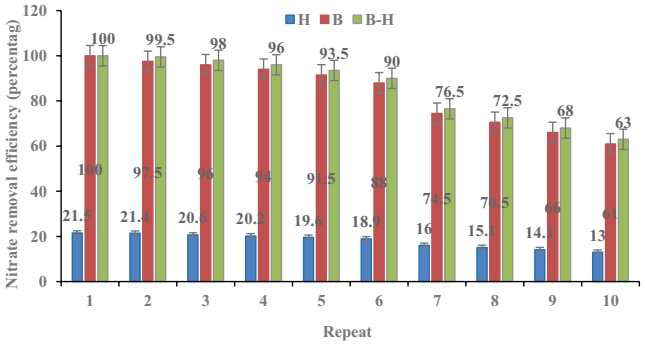

Fig. 10. Effect of adsorbent reusability on NO_3^- removal (optimum conditions: 2 g/dL of adsorbent of clay nanoparticles, reaction time of 60 min, 25 mg/L of NO_3^-, and pH 4). Notes: The reaction time in bentonite adsorbent (B), cationic surfactant (HDTMA-Br) (H) and clay activated using cationic surfactant (HDTMA-Br) (B-H) is 60, 60 and 30 min, respectively.

Table 9
Parameters extracted from NO_3^- adsorption isotherms (linear and non-linear isotherm models)

No.	Isotherm model	Parameter	Value
1	Langmuir	Correlation coefficient	0.996
		Process type (R_L)	0.016
		Equilibrium constant (K_L) (L/mg)	1.16
		Maximum adsorption capacity (q_{max}) (mg/g)	94.33
		RMSE	0.21
2	Freundlich	Coefficient of determination (R^2)	0.927
		Freundlich's constant (n)	3.04
		Freundlich's constant (K_p) (L/mg)(mg/g)	43.51
		RMSE	0.16

equilibrium isotherm and the adsorption capacity was 171.76 mg/g [54].

3.9. Adsorption kinetics

Examining the first-order and second-order kinetic models about the NO_3^- adsorption process and predicting its speed can play an effective role in describing the surface adsorption process [55]. The first-order kinetic coefficient is a correlation coefficient of 0.9268 with a kinetic constant of 0.28. The direct relationship between the changes in NO_3^- solution anions removal, saturation concentration and adsorbent removal; and time is one of the assumptions of first-order adsorption kinetics (Table 10). The second-order kinetic coefficient is a correlation coefficient of 0.9988 with a kinetic constant of 0.01. The adsorption process follows quadratic kinetics and predicts experimental results. The mechanism of NO_3^- adsorption by clay nanoparticles functionalized using cationic surfactant (H) is a chemical adsorption and according to the FTIR results is van der Waals force, electrostatic force or hydrogen bonds between the layers of montmorillonite. The most important design factor of these models is the prediction of the rate of the adsorption process, which kinetic calculation is associated with the control of the reaction dimensions, such as the time required for the adsorbed material to be placed on the adsorbent surface. Correlation coefficient is suitable for judging the choice of kinetic model. For the second-order kinetics, NO_3^- anion adsorption on clay nanoparticle adsorbent functionalized using cationic surfactant H is dependent on NO_3^- concentration. NO_3^- adsorption by clay nanoparticle adsorbent functionalized using cationic surfactant H follows the chemical adsorption type and therefore follows the second-order kinetic model. The laboratory data of NO_3^- adsorption by local green montmorillonite adsorbent follows the second-order model kinetics of adsorption [56]. The laboratory data of NO_3^- adsorption by clay-phosphoric acid-microwave radiation and kaolin-lime-microwave radiation adsorbents followed the pseudo-second-order model kinetics of adsorption [57]. Adsorption performance the amount of NO_3^- anions absorbed at equilibrium can be expressed as q_e (mg/g). Methylene blue onto modified Tamazert kaolin, followed the pseudo-second-order model kinetics of adsorption [58]. Maximum adsorption of methyl orange on chitosan-based composite fibrous adsorbent was 175.45 mg/g [59].

3.10. Ion selectivity study

Fig. 11 shows the effect of anions selectivity such as chloride (Cl^-) of 200 mg/L), sulfate (SO_4^{-2}) of 200 mg/L, and phosphate (PO_4^{-3}) of 200 mg/L on the NO_3^- removal efficiency of 25 mg/L by clay nanoparticles functionalized using cationic surfactant (H) adsorbent. NO_3^- removal efficiency in the presence of 200 mg/L Cl^-, 200 mg/L SO_4^{-2}, and 200 mg/L PO_4^{-3} decreased from 100% to 66.3%, 31.2%, and 98.5%, respectively. The effect of Cl^- and SO_4^{-2} anions is more than PO_4^{-3} due to the greater affinity to ion exchange reaction with the quaternary ammonium group. The production of $H_2PO_4^-$ anion from PO_4^{-3} in acidic conditions and its magnitude lead to the unwillingness of $H_2PO_4^-$ anion to compete with NO_3^- due to the same capacity.

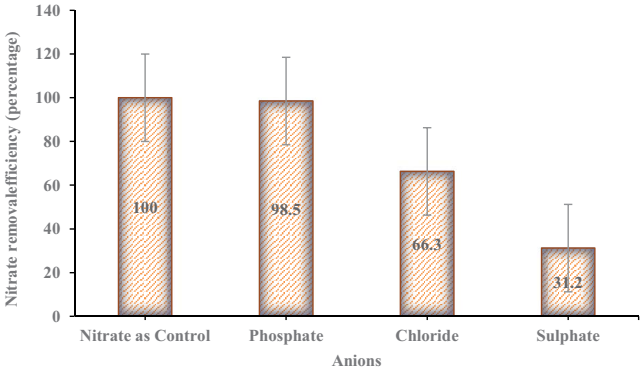

Fig. 11. Effect of anions selectivity (Cl^-) of 200 mg/L, SO_4^{-2} of 200 mg/L, and PO_4^{-3} of 200 mg/L on the NO_3^- removal efficiency of 25 mg/L (optimum conditions: 2 g/dL of adsorbent of clay nanoparticles, reaction time of 60 min, and pH 4).

Table 10
Variables extracted from NO_3^- adsorption kinetics (linear model and non-linear model)

Model	Kinetics reactions	Parameter	Value
Linear	First-order	Correlation coefficient	0.9268
		First-order kinetic constant (g/mg·min)	0.28
		Amount of NO_3^- absorbed at equilibrium (q_e) (mg/g)	20.05
	Second-order	Coefficient of determination (R^2)	0.9988
		Second-order kinetic constant (g/mg·min)	0.01
		Amount of NO_3^- absorbed at equilibrium (q_e) (mg/g)	48.7
Non-linear	First-order	Correlation coefficient	0.9193
		First-order kinetic constant (g/mg·min)	0.91
		Amount of NO_3^- absorbed at equilibrium (q_e) (mg/g)	25.75
	Second-order	Coefficient of determination (R^2)	0.9886
		Second-order kinetic constant (g/mg·min)	1.75
		Amount of NO_3^- absorbed at equilibrium (q_e) (mg/g)	47.60

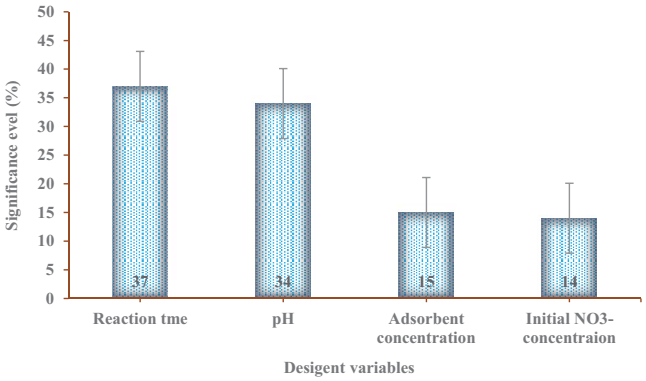

Fig. 12. The Taguchi model (Experimental conditions: temperature: 20°C, pH: 4–9, reaction time: 0–60 min, initial concentration: 25–75 mg/L, adsorbent concentration: 1–3 g/dL).

3.11. Optimization

The Taguchi model was used to determine the optimal operational variable values. Taguchi model results for NO_3^- removal efficiency indicate that reaction time (37%) and initial concentration (14%) are the most significant and the least significant variable, respectively (Fig. 12).

4. Conclusion

The present study was conducted with the aim of absorbing NO_3^- anion as one of the most harmful pollutants from the water environment using batch system of clay nanoparticles functionalized with HDTMA-Br cationic surfactant.

The lower consumption of cationic surfactant and increasing the interlayer surface area compared to other studies are innovations of the current study method. The morphological characteristics of the adsorbents were analyzed using SEM equipped with EDS, XRD and FTIR, which indicated the presence of functional groups and proper performance of the adsorbent. The FTIR results showed that there were van der Waals force, electrostatic force or hydrogen bonds between the layers of montmorillonite. The presence of interlayer spaces could be increased by cationic surfactants due to exchanging cations with the surface in the nanoclay layers which increased the adsorption sites. The result showed that the best optimal conditions and the highest adsorption rate were obtained at pH equal to 4, initial NO_3^- concentrations of 25 mg/L, contact time of less than 15 min, concentration of 1 g/dL of the adsorbent, temperature of 20°C, and adsorbent reusability of at least 4 times was economical due to the with high removal efficiency. The equilibrium isotherms showed that NO_3^- ion adsorption followed the Langmuir equilibrium model ($R^2 = 0.996$), the NO_3^- adsorption capacity is 94.33 mg/g. The results of the kinetic modeling demonstrated that second-order kinetics model ($R^2 = 0.9988$) were found as the best-fitted models. The mechanism of NO_3^- adsorption by clay nanoparticles functionalized using cationic surfactant (H) was a chemical adsorption. The results showed that the modified nanoclay adsorbent is a suitable, cheap and efficient method for removing NO_3^- from drinking water. In terms of implementation, nanoclay adsorbent modified with the organic surfactant HDTMA-Br was used as a strong adsorbent to remove NO_3^- from aqueous media due to its high adsorption capacity and reusability for at least 4 cycles of recycling. In terms of practical and a concluding remark, the nanoclay adsorbent modified with the organic surfactant HDTMA-Br can be used as a purification process at the point of use to treat NO_3^--contaminated water. Investigating the removal efficiency of NO_3^- by the nanoclay adsorbent modified with the organic surfactant HDTMA-Br in the presence of other anions and other cations in water is suggested for future research.

Acknowledgements

This article is taken from the master's thesis "Investigation of Nitrate and Chloride Removal Efficiency by Clay Nanoparticles Adsorbent Functionalized using Cationic Surfactant" with the code of ethics IR.IAU.TMU.REC.1400.085. Hereby, the authors acknowledge laboratory support of Environmental Health Engineering Department and Water Purification Research Center of Tehran Islamic Azad University of Medical Sciences.

Conflict of interests

The authors of this article declare that they have no conflict of interests.

References

[1] M. Preisner, Surface water pollution by untreated municipal wastewater discharge due to a sewer failure, Environ. Processes, 7 (2020) 767–780.
[2] M. Radfarda, A. Gholizadehc, A. Azhdarpoorb, A. Badeenezhada, A.A. Mohammadid, M. Yousefie, Health risk assessment to fluoride and nitrate in drinking water of rural residents living in the Bardaskan city, arid region, southeastern Iran, Desal. Water Treat., 145 (2019) 249–256.
[3] M. Malakotian, H. Hashemi, New methods analysis of nitrate removal from water resources, Tolooebehdasht, 13 (2015) 11–24.
[4] J. Lu, Z. Bai, G.L. Velthof, Z. Wu, D. Chadwick, L. Ma, Accumulation and leaching of nitrate in soils in wheat-maize production in China, Agric. Water Manage., 212 (2019) 407–415.
[5] H. Godini, A. Rezaee, F. Beyranvand, N. Jahanbani, Nitrate removal from water using denitrifier-bacteria immobilized on activated carbon at fluidized-bed reactor, Sci. Mag. yafte, 14 (2012) 15–27.
[6] M. Parvizishad, A. Dalvand, A.H. Mahvi, F. Goodarzi, A review of adverse effects and benefits of nitrate and nitrite in drinking water and food on human health, Health Scope, 6 (2017) e14164, doi: 10.5812/jhealthscope.14164.
[7] A. Azhdarpoor, M. Radfard, M. Pakdel, A. Abbasnia, A. Badeenezhad, A.A. Mohammadi, M. Yousefi, Assessing fluoride and nitrate contaminants in drinking water resources and their health risk assessment in a semiarid region of southwest Iran, Desal. Water Treat., 149 (2019) 43–51.
[8] P. Juntakut, E.M.K. Haacker, D.D. Snow, C. Ray, Risk and cost assessment of nitrate contamination in domestic wells, Water, 12 (2020) 428, doi: 10.3390/w12020428.
[9] M. Alimohammadi, N. Latifi, R. Nabizadeh, K. Yaghmaeian, A.H. Mahvi, M. Yousefi, P. Foroohar, S. Hemmati, Z. Heidarinejad, Determination of nitrate concentration and its risk assessment in bottled water in Iran, Data Brief, 19 (2018) 2133–2138.
[10] S. Tyagi, D. Rawtani, N. Khatri, M. Tharmavaram, Strategies for nitrate removal from aqueous environment using

nanotechnology: a review, J. Water Process Eng., 21 (2018) 84–95.
[11] A. Hekmatzadeh, A. Karimi-Jashani, N. Talebbeydokhti, B. Kløve, Modeling of nitrate removal for ion exchange resin in batch and fixed bed experiments, Desalination, 284 (2012) 22–31.
[12] A.A. Babaei, K. Ahmadi, I. Kazeminezhad, S.N. Alavi, A. Takdastan, Synthesis and application of magnetic hydroxyapatite for removal of tetracycline from aqueous solutions, J. Mazandaran Univ. Med. Sci., 26 (2016) 146–159.
[13] N. Singh, G. Nagpal, S. Agrawal, Water purification by using adsorbents: a review, Environ. Technol. Innovation, 11 (2018) 187–240.
[14] M.R. Awual, M.M. Hasan, A. Islam, M.M. Rahman, A.M. Asiri, M.A. Khaleque, M.C. Sheikh, Introducing an amine functionalized novel conjugate material for toxic nitrite detection and adsorption from wastewater, J. Cleaner Prod., 228 (2019) 778–785.
[15] M.R. Awual, Efficient phosphate removal from water for controlling eutrophication using novel composite adsorbent, J. Cleaner Prod., 228 (2019) 1311–1319.
[16] M.R. Awual, M.M. Hasan, A.M. Asiri, M.M. Rahman, Cleaning the arsenic(V) contaminated water for safe-guarding the public health using novel composite material, Composites, Part B, 171 (2019) 294–301.
[17] R.M. Kamel, A. Shahat, W.H. Hegazy, E.M. Khodier, M.R. Awual, Efficient toxic nitrite monitoring and removal from aqueous media with ligand based conjugate materials, J. Mol. Liq., 285 (2019) 20–26.
[18] M.R. Awual, T. Yaita, S. Suzuki, H. Shiwaku, Ultimate selenium(IV) monitoring and removal from water using a new class of organic ligand based composite adsorbent, J. Hazard. Mater., 291 (2015) 111–119.
[19] B. Biswas, L.N. Warr, E.F. Hilder, N. Goswami, M.M. Rahman, J.G. Churchman, K. Vasilev, G. Pan, R. Naidu, Biocompatible functionalisation of nanoclays for improved environmental remediation, Chem. Soc. Rev., 48 (2019) 3740–3770.
[20] F.O. Nwosu, O.J. Ajala, R.M. Owoyemi, B.G. Raheem, Preparation and characterization of adsorbents derived from bentonite and kaolin clays, Appl. Water Sci., 8 (2018) 1–10.
[21] M. Enkari, E. Ebrahimi Aghmasjed, Removal of nitrate ion from aqueous solution using octa decyl amine modified montmorillonite nanoclay, Environ. Water Eng., 4 (2019) 286–298.
[22] J.-K. Kang, S.-C. Lee, S.-B. Kim, Synthesis of quaternary ammonium-functionalized silica gel through grafting of dimethyl dodecyl [3-(trimethoxysilyl) propyl] ammonium chloride for nitrate removal in batch and column studies, J. Taiwan Inst. Chem. Eng., 102 (2019) 153–162.
[23] L. El Hanache, L. Sundermann, B. Lebeau, J. Toufaily, T. Hamieh, T.J. Daou, Surfactant-modified MFI-type nanozeolites: super-adsorbents for nitrate removal from contaminated water, Microporous Mesoporous Mater., 283 (2019) 1–13.
[24] P. Singla, R. Mehta, S.N. Upadhyay, Clay modification by the use of organic cations, Green Sustainable Chem., 2 (2012) 21–25.
[25] A. Motawie, M. Madany, A. El-Dakrory, H. Osman, E. Ismail, M. Badr, D. El-Komy, D. Abulyazied, Physico-chemical characteristics of nano-organo bentonite prepared using different organo-modifiers, Egypt. J. Pet., 23 (2014) 331–338.
[26] Z. Ansari-Asl, Z. Neisi, T. Sedaghat, V. Nobakht, Synthesis, characterization, and electrochemical properties of polyaniline/Co(II) metal-organic framework composites, Appl. Chem., 14 (2019) 251–266.
[27] A.M. Hassan, W.A.W. Ibrahim, M.B. Bakar, M.M. Sanagi, Z.A. Sutirman, H.R. Nodeh, M.A. Mokhter, New effective 3-aminopropyltrimethoxysilane functionalized magnetic sporopollenin-based silica coated graphene oxide adsorbent for removal of Pb(II) from aqueous environment, J. Environ. Manage., 253 (2020) 109658, doi: 10.1016/j.jenvman.2019.109658.
[28] S.I. Rathnayake, Y. Xi, R.L. Frost, G.A. Ayoko, Environmental applications of inorganic–organic clays for recalcitrant organic pollutants removal: bisphenol A, J. Colloid Interface Sci., 470 (2016) 183–195.
[29] H. Long, P. Wu, N. Zhu, Evaluation of Cs^+ removal from aqueous solution by adsorption on ethylamine-modified montmorillonite, Chem. Eng. J., 225 (2013) 237–244.
[30] G.B.B. Varadwaj, S. Rana, K. Parida, Amine functionalized K10 montmorillonite: a solid acid–base catalyst for the Knoevenagel condensation reaction, Dalton Trans., 42 (2013) 5122–5129.
[31] M.A. Jaworski, F.M. Flores, M.A. Fernández, M. Casella, R.M. Torres Sánchez, Use of organo-montmorillonite for the nitrate retention in water: influence of alkyl length of loaded surfactants, SN Appl. Sci., 1 (2019) 1–9.
[32] M.M. Hasan, M.S. Salman, M.N. Hasan, A.I. Rehan, M.E. Awual, A.I. Rasee, R. Waliullah, M.S. Hossain, K.T. Kubra, M.C. Sheikh, Facial conjugate adsorbent for sustainable Pb(II) ion monitoring and removal from contaminated water, Colloids Surf., A, 673 (2023) 131794, doi: 10.1016/j.colsurfa.2023.131794.
[33] A.S. Mahmoud, Effect of nano bentonite on direct yellow 50 dye removal; adsorption isotherm, kinetic analysis, and thermodynamic behavior, Prog. React. Kinet. Mech., 47 (2022) 14686783221090377, doi: 10.1177/14686783221090377.
[34] E.A. Khodaeer, Removal of direct 50 dyes from aqueous solution using natural clay and organoclay adsorbents, Baghdad Sci. J., 12 (2015) 157–166.
[35] M.R. Awual, M.N. Hasan, M.M. Hasan, M.S. Salman, M.C. Sheikh, K.T. Kubra, M.S. Islam, H.M. Marwani, A. Islam, M.A. Khaleque, Green and robust adsorption and recovery of Europium(III) with a mechanism using hybrid donor conjugate materials, Sep. Purif. Technol., 319 (2023) 124088, doi: 10.1016/j.seppur.2023.124088.
[36] A. Maged, S. Kharbish, I.S. Ismael, A. Bhatnagar, Characterization of activated bentonite clay mineral and the mechanisms underlying its sorption for ciprofloxacin from aqueous solution, Environ. Sci. Pollut. Res., 27 (2020) 32980–32997.
[37] M. El Ouardi, S. Qourzal, S. Alahiane, A. Assabbane, J. Douch, Effective removal of nitrates ions from aqueous solution using new clay as potential low-cost adsorbent, J. Encapsulation Adsorpt. Sci., 5 (2015) 178–190.
[38] S. Çoruh, F. Geyikci, Adsorption of copper(II) ions on montmorillonite and sepiolite clays: equilibrium and kinetic studies, Desal. Water Treat., 45 (2012) 351–360.
[39] J.K. Mbadcam, S. Dongmo, D. Dinka'a Ndaghu, Kinetic and thermodynamic studies of the adsorption of nickel(II) ions from aqueous solutions by smectite clay from Sabga–Cameroon, Int. J. Curr. Res., 4 (2012) 162–167.
[40] K.T. Kubra, M.M. Hasan, M.N. Hasan, M.S. Salman, M.A. Khaleque, M.C. Sheikh, A.I. Rehan, A.I. Rasee, R. Waliullah, M.E. Awual, The heavy lanthanide of Thulium(III) separation and recovery using specific ligand-based facial composite adsorbent, Colloids Surf., A, 667 (2023) 131415, doi: 10.1016/j.colsurfa.2023.131415.
[41] U.A. Guler, M. Sarioglu, Single and binary biosorption of Cu(II), Ni(II) and methylene blue by raw and pretreated *Spirogyra* sp.: equilibrium and kinetic modeling, J. Environ. Chem. Eng., 1 (2013) 369–377.
[42] A. Bafkar, N. Baboli, Investigation of the efficiency of nitrate removal from aqueous solution using oak leaf nanostructure adsorbent, J. Soil Water Conserv., 25 (2018) 233–247.
[43] M.S. Salman, M.C. Sheikh, M.M. Hasan, M.N. Hasan, K.T. Kubra, A.I. Rehan, M.E. Awual, A.I. Rasee, R. Waliullah, M.S. Hossain, Chitosan-coated cotton fiber composite for efficient toxic dye encapsulation from aqueous media, Appl. Surf. Sci., 622 (2023) 157008, doi: 10.1016/j.apsusc.2023.157008.
[44] K. Yahya, W. Hamdi, N. Hamdi, Organoclay Nano-Adsorbent: Preparation, Characterization and Applications, W. Oueslati, Ed., Nanoclay-Recent Advances, New Perspectives and Applications, IntechOpen, 2022.
[45] M. Shirzad-Siboni, A. Khataee, A. Hassani, S. Karaca, Preparation, characterization and application of a CTAB-modified nanoclay for the adsorption of an herbicide from aqueous solutions: kinetic and equilibrium studies, C.R. Chim., 18 (2015) 204–214.

[46] L. Zhang, B. Zhang, T. Wu, D. Sun, Y. Li, Adsorption behavior and mechanism of chlorophenols onto organoclays in aqueous solution, Colloids Surf., A, 484 (2015) 118–129.
[47] M. Saeed, A. Riaz, A. Intisar, M. Iqbal Zafar, H. Fatima, H. Howari, A. Alhodaib, A. Waseem, Synthesis, characterization and application of organoclays for adsorptive desulfurization of fuel oil, Sci. Rep., 12 (2022) 7362, doi: 10.1038/s41598-022-11054-6.
[48] S. Ullah, S. Hussain, W. Ahmad, H. Khan, K.I. Khan, S.U. Khan, S. Khan, Desulfurization of model oil through adsorption over activated charcoal and bentonite clay composites, Chem. Eng. Technol., 43 (2020) 564–573.
[49] E.C. Lima, A. Hosseini-Bandegharaei, J.C. Moreno-Piraján, I. Anastopoulos, A critical review of the estimation of the thermodynamic parameters on adsorption equilibria. Wrong use of equilibrium constant in the Van't Hoof equation for calculation of thermodynamic parameters of adsorption, J. Mol. Liq., 273 (2019) 425–434.
[50] M.S. Salman, M.N. Hasan, M.M. Hasan, K.T. Kubra, M.C. Sheikh, A.I. Rehan, R. Waliullah, A.I. Rasee, M.E. Awual, M.S. Hossain, Improving copper(II) ion detection and adsorption from wastewater by the ligand-functionalized composite adsorbent, J. Mol. Struct., 1282 (2023) 135259, doi: 10.1016/j.molstruc.2023.135259.
[51] I.H. Khalaf, F.T. Al-Sudani, A.A. AbdulRazak, T. Aldahri, S. Rohani, Optimization of Congo red dye adsorption from wastewater by a modified commercial zeolite catalyst using response surface modeling approach, Water Sci. Technol., 83 (2021) 1369–1383.
[52] A. Battas, A.E. Gaidoumi, A. Ksakas, A. Kherbeche, Adsorption study for the removal of nitrate from water using local clay, Sci. World J., 2019 (2019) 9529618, doi: 10.1155/2019/9529618.
[53] H. Masoudi, F. Ravari, H. Mosaddeghi, Removal of nitrate from water by modified nano-clay and comparison with nano-graphene, nano-Fe_3O_4 and nano-clay-isotherm and kinetic studies, Desal. Water Treat., 167 (2019) 218–230.
[54] M.N. Hasan, M.S. Salman, M.M. Hasan, K.T. Kubra, M.C. Sheikh, A.I. Rehan, A.I. Rasee, M.E. Awual, R. Waliullah, M.S. Hossain, Assessing sustainable Lutetium(III) ions adsorption and recovery using novel composite hybrid nanomaterials, J. Mol. Struct., 1276 (2023) 134795, doi: 10.1016/j.molstruc.2022.134795.
[55] D. Kavitha, C. Namasivayam, Experimental and kinetic studies on methylene blue adsorption by coir pith carbon, Bioresour. Technol., 98 (2007) 14–21.
[56] A.S. Fazlzadeh, M. Vosoughi, R. Khosravi, A. Sadigh, Nitrate ion adsorption from aqueous solution by a novel local green montmorillonite adsorbent, J. Health, 8 (2017) 298–311.
[57] B. Hamouda, M. Kemiha, N. Azzouz, Effective removal of nitrate ions from aqueous solution using new clays: Tamazert kaolin treated under microwave irradiation, Desal. Water Treat., 155 (2019) 321–328.
[58] A. Boukhemkhem, K. Rida, Improvement adsorption capacity of methylene blue onto modified Tamazert kaolin, Adsorpt. Sci. Technol., 35 (2017) 753–773.
[59] A.I. Rehan, A.I. Rasee, M.E. Awual, R. Waliullah, M.S. Hossain, K.T. Kubra, M.S. Salman, M.M. Hasan, M.N. Hasan, M.C. Sheikh, Improving toxic dye removal and remediation using novel nanocomposite fibrous adsorbent, Colloids Surf., A, 673 (2023) 131859, doi: 10.1016/j.colsurfa.2023.131859.